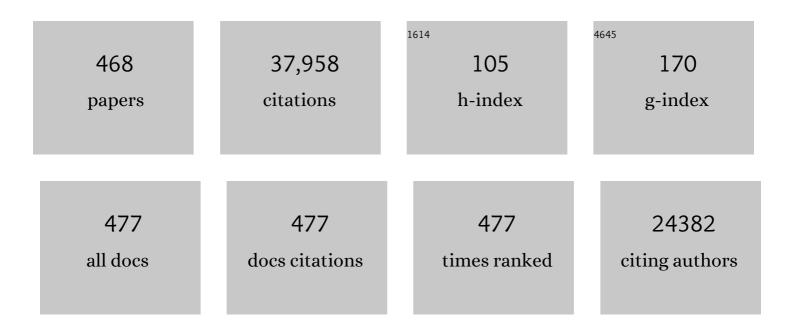
List of Publications by Year in descending order

Source: https://exaly.com/author-pdf/11860499/publications.pdf Version: 2024-02-01



#	Article	IF	CITATIONS
1	Structure and process relationship of electrospun bioabsorbable nanofiber membranes. Polymer, 2002, 43, 4403-4412.	3.8	1,671
2	Functional electrospun nanofibrous scaffolds for biomedical applications. Advanced Drug Delivery Reviews, 2007, 59, 1392-1412.	13.7	861
3	Incorporation and controlled release of a hydrophilic antibiotic using poly(lactide-co-glycolide)-based electrospun nanofibrous scaffolds. Journal of Controlled Release, 2004, 98, 47-56.	9.9	707
4	Electrospun fine-textured scaffolds for heart tissue constructs. Biomaterials, 2005, 26, 5330-5338.	11.4	597
5	NANOFIBROUS MATERIALS AND THEIR APPLICATIONS. Annual Review of Materials Research, 2006, 36, 333-368.	9.3	573
6	Control of degradation rate and hydrophilicity in electrospun non-woven poly(d,l-lactide) nanofiber scaffolds for biomedical applications. Biomaterials, 2003, 24, 4977-4985.	11.4	524
7	High flux ultrafiltration membranes based on electrospun nanofibrous PAN scaffolds and chitosan coating. Polymer, 2006, 47, 2434-2441.	3.8	503
8	Structure Development during Shear Flow-Induced Crystallization of i-PP:  In-Situ Small-Angle X-ray Scattering Study. Macromolecules, 2000, 33, 9385-9394.	4.8	465
9	Flow-induced shish-kebab precursor structures in entangled polymer melts. Polymer, 2005, 46, 8587-8623.	3.8	427
10	Functional nanofibers for environmental applications. Journal of Materials Chemistry, 2008, 18, 5326.	6.7	388
11	Crystallization Temperature-Dependent Crystal Orientations within Nanoscale Confined Lamellae of a Self-Assembled Crystallineâ^Amorphous Diblock Copolymer. Journal of the American Chemical Society, 2000, 122, 5957-5967.	13.7	387
12	Structure Development during Shear Flow Induced Crystallization of i-PP:Â In Situ Wide-Angle X-ray Diffraction Study. Macromolecules, 2001, 34, 5902-5909.	4.8	385
13	Antithrombogenic property of bone marrow mesenchymal stem cells in nanofibrous vascular grafts. Proceedings of the National Academy of Sciences of the United States of America, 2007, 104, 11915-11920.	7.1	360
14	Small-Angle X-ray Scattering of Polymers. Chemical Reviews, 2001, 101, 1727-1762.	47.7	348
15	High Flux Filtration Medium Based on Nanofibrous Substrate with Hydrophilic Nanocomposite Coating. Environmental Science & Technology, 2005, 39, 7684-7691.	10.0	348
16	Bioactive Nanofibers:Â Synergistic Effects of Nanotopography and Chemical Signaling on Cell Guidance. Nano Letters, 2007, 7, 2122-2128.	9.1	339
17	Isothermal Crystallization of Poly(<scp>I</scp> -lactide) Induced by Graphene Nanosheets and Carbon Nanotubes: A Comparative Study. Macromolecules, 2010, 43, 5000-5008.	4.8	308
18	Electro-Spinning and Electro-Blowing of Hyaluronic Acid. Biomacromolecules, 2004, 5, 1428-1436.	5.4	300

#	Article	IF	CITATIONS
19	Myotube Assembly on Nanofibrous and Micropatterned Polymers. Nano Letters, 2006, 6, 537-542.	9.1	293
20	Orientation and Crystallization of Natural Rubber Network As Revealed by WAXD Using Synchrotron Radiation. Macromolecules, 2004, 37, 3299-3309.	4.8	273
21	Polymeric nanostructured materials for biomedical applications. Progress in Polymer Science, 2016, 60, 86-128.	24.7	257
22	Unexpected Shish-Kebab Structure in a Sheared Polyethylene Melt. Physical Review Letters, 2005, 94, 117802.	7.8	254
23	Optimization and Characterization of Dextran Membranes Prepared by Electrospinning. Biomacromolecules, 2004, 5, 326-333.	5.4	253
24	Electrospun nanofibrous membranes for high flux microfiltration. Journal of Membrane Science, 2012, 392-393, 167-174.	8.2	253
25	Effects of organoclays on morphology and thermal and rheological properties of polystyrene and poly(methyl methacrylate) blends. Journal of Polymer Science, Part B: Polymer Physics, 2003, 41, 44-54.	2.1	250
26	Ultra-fine cellulose nanofibers: new nano-scale materials for water purification. Journal of Materials Chemistry, 2011, 21, 7507.	6.7	250
27	Micro-nano structure poly(ether sulfones)/poly(ethyleneimine) nanofibrous affinity membranes for adsorption of anionic dyes and heavy metal ions in aqueous solution. Chemical Engineering Journal, 2012, 197, 88-100.	12.7	250
28	Structure and Morphology Changes during in Vitro Degradation of Electrospun Poly(glycolide-co-lactide) Nanofiber Membrane. Biomacromolecules, 2003, 4, 416-423.	5.4	248
29	New Insights into Structural Development in Natural Rubber during Uniaxial Deformation by In Situ Synchrotron X-ray Diffraction. Macromolecules, 2002, 35, 6578-6584.	4.8	242
30	High flux nanofiltration membranes based on interfacially polymerized polyamide barrier layer on polyacrylonitrile nanofibrous scaffolds. Journal of Membrane Science, 2009, 326, 484-492.	8.2	237
31	In-Situ Studies of Structure Development during Deformation of a Segmented Poly(urethaneâ^'urea) Elastomer. Macromolecules, 2003, 36, 1940-1954.	4.8	236
32	Temperature dependence of polymer crystalline morphology in nylon 6/montmorillonite nanocomposites. Polymer, 2001, 42, 09975-09985.	3.8	234
33	High performance ultrafiltration composite membranes based on poly(vinyl alcohol) hydrogel coating on crosslinked nanofibrous poly(vinyl alcohol) scaffold. Journal of Membrane Science, 2006, 278, 261-268.	8.2	225
34	Mineralization of hydroxyapatite in electrospun nanofibrous poly(L-lactic acid) scaffolds. Journal of Biomedical Materials Research - Part A, 2006, 79A, 307-317.	4.0	220
35	Shear-Induced Precursor Structures in Isotactic Polypropylene Melt by in-Situ Rheo-SAXS and Rheo-WAXD Studies. Macromolecules, 2002, 35, 9096-9104.	4.8	219
36	Shear-Enhanced Crystallization in Isotactic Polypropylene. 3. Evidence for a Kinetic Pathway to Nucleation. Macromolecules, 2002, 35, 1762-1769.	4.8	217

#	Article	IF	CITATIONS
37	Nanofibrous microfiltration membranes capable of removing bacteria, viruses and heavy metal ions. Journal of Membrane Science, 2013, 446, 376-382.	8.2	215
38	Ultrafine Polysaccharide Nanofibrous Membranes for Water Purification. Biomacromolecules, 2011, 12, 970-976.	5.4	212
39	Thiol-modified cellulose nanofibrous composite membranes for chromium (VI) and lead (II) adsorption. Polymer, 2014, 55, 1167-1176.	3.8	211
40	Control of structure, morphology and property in electrospun poly(glycolide-co-lactide) non-woven membranes via post-draw treatments. Polymer, 2003, 44, 4959-4967.	3.8	207
41	Nanofibrous Microfiltration Membrane Based on Cellulose Nanowhiskers. Biomacromolecules, 2012, 13, 180-186.	5.4	201
42	Electrospun nanofiber membranes. Current Opinion in Chemical Engineering, 2016, 12, 62-81.	7.8	200
43	Shear-Induced Crystallization Precursor Studies in Model Polyethylene Blends by in-Situ Rheo-SAXS and Rheo-WAXD. Macromolecules, 2004, 37, 4845-4859.	4.8	197
44	Ultrafine Cellulose Nanofibers as Efficient Adsorbents for Removal of UO ₂ ²⁺ in Water. ACS Macro Letters, 2012, 1, 213-216.	4.8	187
45	Nanoscale reinforcement of polyhedral oligomeric silsesquioxane (POSS) in polyurethane elastomer. Polymer International, 2000, 49, 437-440.	3.1	182
46	Hard and soft confinement effects on polymer crystallization in microphase separated cylinder-forming PEO-b-PS/PS blends. Polymer, 2001, 42, 9121-9131.	3.8	179
47	Shear-Induced Molecular Orientation and Crystallization in Isotactic Polypropylene: Effects of the Deformation Rate and Strain. Macromolecules, 2005, 38, 1244-1255.	4.8	179
48	Prevention of Postsurgery-Induced Abdominal Adhesions by Electrospun Bioabsorbable Nanofibrous Poly(lactide-co-glycolide)-Based Membranes. Annals of Surgery, 2004, 240, 910-915.	4.2	178
49	The role of interlamellar chain entanglement in deformation-induced structure changes during uniaxial stretching of isotactic polypropylene. Polymer, 2007, 48, 6867-6880.	3.8	173
50	Structure, crystallization and morphology of poly (aryl ether ketone ketone). Polymer, 1992, 33, 2483-2495.	3.8	172
51	Structural and Morphological Studies of Isotactic Polypropylene Fibers during Heat/Draw Deformation by in-Situ Synchrotron SAXS/WAXD. Macromolecules, 2001, 34, 2569-2578.	4.8	172
52	Improved barrier properties of poly(lactic acid) with randomly dispersed graphene oxide nanosheets. Journal of Membrane Science, 2014, 464, 110-118.	8.2	170
53	Formation and Stability of Shear-Induced Shish-Kebab Structure in Highly Entangled Melts of UHMWPE/HDPE Blends. Macromolecules, 2008, 41, 4766-4776.	4.8	162

54 Crystal Orientation Changes in Two-Dimensionally Confined Nanocylinders in a Poly(ethylene) Tj ETQq0 0 0 rgBT /Overlock 10 Tf 50 62

#	Article	IF	CITATIONS
55	Physical gelation in ethylene–propylene copolymer melts induced by polyhedral oligomeric silsesquioxane (POSS) molecules. Polymer, 2003, 44, 1499-1506.	3.8	160
56	Graphene Nanosheets and Shear Flow Induced Crystallization in Isotactic Polypropylene Nanocomposites. Macromolecules, 2011, 44, 2808-2818.	4.8	160
57	Time-resolved X-ray study of poly(aryl ether ether ketone) crystallization and melting behaviour: 1. Crystallization. Polymer, 1993, 34, 3986-3995.	3.8	157
58	Formation of functional polyethersulfone electrospun membrane for water purification by mixed solvent and oxidation processes. Polymer, 2009, 50, 2893-2899.	3.8	156
59	Probing the Early Stages of Melt Crystallization in Polypropylene by Simultaneous Small- and Wide-Angle X-ray Scattering and Laser Light Scattering. Macromolecules, 2000, 33, 978-989.	4.8	154
60	Highly Permeable Polymer Membranes Containing Directed Channels for Water Purification. ACS Macro Letters, 2012, 1, 723-726.	4.8	154
61	Initial-Stage Growth Controlled Crystal Orientations in Nanoconfined Lamellae of a Self-Assembled Crystallineâ^'Amorphous Diblock Copolymer. Macromolecules, 2001, 34, 1244-1251.	4.8	152
62	Effective chromium removal from water by polyaniline-coated electrospun adsorbent membrane. Chemical Engineering Journal, 2019, 372, 341-351.	12.7	151
63	Continuous polymer nanofiber yarns prepared by self-bundling electrospinning method. Polymer, 2008, 49, 2755-2761.	3.8	150
64	Fabrication and characterization of cellulose nanofiber based thin-film nanofibrous composite membranes. Journal of Membrane Science, 2014, 454, 272-282.	8.2	150
65	Unprecedented Access to Strong and Ductile Poly(lactic acid) by Introducing In Situ Nanofibrillar Poly(butylene succinate) for Green Packaging. Biomacromolecules, 2014, 15, 4054-4064.	5.4	149
66	Effect of Nanoclay on Natural Rubber Microstructure. Macromolecules, 2008, 41, 6763-6772.	4.8	144
67	Functionalized electrospun nanofibrous microfiltration membranes for removal of bacteria and viruses. Journal of Membrane Science, 2014, 452, 446-452.	8.2	142
68	Shear-Induced Crystallization in Novel Long Chain Branched Polypropylenes by in Situ Rheo-SAXS and -WAXD. Macromolecules, 2003, 36, 5226-5235.	4.8	141
69	Dual-Biomimetic Superhydrophobic Electrospun Polystyrene Nanofibrous Membranes for Membrane Distillation. ACS Applied Materials & Interfaces, 2014, 6, 2423-2430.	8.0	141
70	Mechanism of strain-induced crystallization in filled and unfilled natural rubber vulcanizates. Journal of Applied Physics, 2005, 97, 103529.	2.5	140
71	Low-dimensional carbonaceous nanofiller induced polymer crystallization. Progress in Polymer Science, 2014, 39, 555-593.	24.7	140
72	Phase transformation in quenched mesomorphic isotactic polypropylene. Polymer, 2001, 42, 7561-7566.	3.8	138

#	Article	IF	CITATIONS
73	High flux ultrafiltration nanofibrous membranes based on polyacrylonitrile electrospun scaffolds and crosslinked polyvinyl alcohol coating. Journal of Membrane Science, 2009, 338, 145-152.	8.2	138
74	Nanocellulose from Spinifex as an Effective Adsorbent to Remove Cadmium(II) from Water. ACS Sustainable Chemistry and Engineering, 2018, 6, 3279-3290.	6.7	138
75	Formation of water-resistant hyaluronic acid nanofibers by blowing-assisted electro-spinning and non-toxic post treatments. Polymer, 2005, 46, 4853-4867.	3.8	136
76	Crystallization studies of isotactic polypropylene containing nanostructured polyhedral oligomeric silsesquioxane molecules under quiescent and shear conditions. Journal of Polymer Science, Part B: Polymer Physics, 2001, 39, 2727-2739.	2.1	135
77	Electrospinning of Hyaluronic Acid (HA) and HA/Gelatin Blends. Macromolecular Rapid Communications, 2006, 27, 114-120.	3.9	134
78	Shear-Enhanced Crystallization in Isotactic Polypropylene. In-Situ Synchrotron SAXS and WAXD. Macromolecules, 2004, 37, 9005-9017.	4.8	132
79	Entanglements and Networks to Strain-Induced Crystallization and Stress–Strain Relations in Natural Rubber and Synthetic Polyisoprene at Various Temperatures. Macromolecules, 2013, 46, 5238-5248.	4.8	132
80	Mesophase as the Precursor for Strain-Induced Crystallization in Amorphous Poly(ethylene) Tj ETQq0 0 0 rgBT /C)verlock 10 4.8) Tf 50 462 T 131
81	Confinement Size Effect on Crystal Orientation Changes of Poly(ethylene oxide) Blocks in Poly(ethylene oxide)-b-polystyrene Diblock Copolymers. Macromolecules, 2004, 37, 3689-3698.	4.8	130
82	Structure and Morphology Changes in Absorbable Poly(glycolide) and Poly(glycolide-co-lactide) during in Vitro Degradation. Macromolecules, 1999, 32, 8107-8114.	4.8	128
83	Competitive Growth of α- and β-Crystals in β-Nucleated Isotactic Polypropylene under Shear Flow. Macromolecules, 2010, 43, 6760-6771.	4.8	128
84	Formation of Shish-Kebabs in Injection-Molded Poly(<scp>l</scp> -lactic acid) by Application of an Intense Flow Field. ACS Applied Materials & amp; Interfaces, 2012, 4, 6774-6784.	8.0	128
85	High-flux microfiltration filters based on electrospun polyvinylalcohol nanofibrous membranes. Polymer, 2013, 54, 548-556.	3.8	128
86	Self-assembly and crystallization behavior of a double-crystalline polyethylene-block-poly(ethylene) Tj ETQq0 0 0	rgBT_/Over	rlock 10 Tf 5 127
87	Patterning Polyethylene Oligomers on Carbon Nanotubes Using Physical Vapor Deposition. Nano Letters, 2006, 6, 1007-1012.	9.1	126
88	Block Copolymers with a Twist. Journal of the American Chemical Society, 2009, 131, 18533-18542.	13.7	126
89	Phase structures and morphologies determined by competitions among self-organization, crystallization, and vitrification in a disordered poly(ethylene oxide)-b-polystyrene diblock copolymer. Physical Review B, 1999, 60, 10022-10031.	3.2	125

90High-flux thin-film nanofibrous composite ultrafiltration membranes containing cellulose barrier
layer. Journal of Materials Chemistry, 2010, 20, 4692.6.7125

#	Article	IF	CITATIONS
91	In-Situ Simultaneous Synchrotron Small- and Wide-Angle X-ray Scattering Measurement of Poly(vinylidene fluoride) Fibers under Deformation. Macromolecules, 2000, 33, 1765-1777.	4.8	124
92	Perforated Layer Structures in Liquid Crystalline Rodâ^ Coil Block Copolymers. Journal of the American Chemical Society, 2005, 127, 15481-15490.	13.7	124
93	A Simple Approach to Prepare Carboxycellulose Nanofibers from Untreated Biomass. Biomacromolecules, 2017, 18, 2333-2342.	5.4	124
94	Structure Study of Cellulose Fibers Wet-Spun from Environmentally Friendly NaOH/Urea Aqueous Solutions. Biomacromolecules, 2007, 8, 1918-1926.	5.4	121
95	Molecular orientation and structural development in vulcanized polyisoprene rubbers during uniaxial deformation by in situ synchrotron X-ray diffraction. Polymer, 2003, 44, 6003-6011.	3.8	120
96	Nanocelluloseâ€Enabled Membranes for Water Purification: Perspectives. Advanced Sustainable Systems, 2020, 4, 1900114.	5.3	118
97	Electrospun polystyrene nanofibrous membranes for direct contact membrane distillation. Journal of Membrane Science, 2016, 515, 86-97.	8.2	114
98	Characterization of Nanocellulose Using Small-Angle Neutron, X-ray, and Dynamic Light Scattering Techniques. Journal of Physical Chemistry B, 2017, 121, 1340-1351.	2.6	112
99	Deformation-Induced Phase Transition and Superstructure Formation in Poly(ethylene terephthalate). Macromolecules, 2005, 38, 91-103.	4.8	111
100	Development of hydrophilic barrier layer on nanofibrous substrate as composite membrane via a facile route. Journal of Membrane Science, 2010, 356, 110-116.	8.2	111
101	High performance thin-film nanofibrous composite hemodialysis membranes with efficient middle-molecule uremic toxin removal. Journal of Membrane Science, 2017, 523, 173-184.	8.2	111
102	Glass transition, crystallization, and morphology relationships in miscible poly(aryl ether ketones) and poly(ether imide) blends. Journal of Polymer Science, Part B: Polymer Physics, 1993, 31, 901-915.	2.1	110
103	Time-resolved X-ray study of poly(aryl ether ether ketone) crystallization and melting behaviour: 2. Melting. Polymer, 1993, 34, 3996-4003.	3.8	110
104	Nanofiltration membranes prepared by interfacial polymerization on thin-film nanofibrous composite scaffold. Polymer, 2014, 55, 1358-1366.	3.8	109
105	Precursors of primary nucleation induced by flow in isotactic polypropylene. Physica A: Statistical Mechanics and Its Applications, 2002, 304, 145-157.	2.6	107
106	X-ray studies of regenerated cellulose fibers wet spun from cotton linter pulp in NaOH/thiourea aqueous solutions. Polymer, 2006, 47, 2839-2848.	3.8	107
107	New insights into the relationship between network structure and strain-induced crystallization in un-vulcanized and vulcanized natural rubber by synchrotron X-ray diffraction. Polymer, 2009, 50, 2142-2148.	3.8	107
108	Nanofibrous polydopamine complex membranes for adsorption of Lanthanum (III) ions. Chemical Engineering Journal, 2014, 244, 307-316.	12.7	106

#	Article	IF	CITATIONS
109	Time-resolved shear behavior of end-tethered Nylon 6–clay nanocomposites followed by non-isothermal crystallization. Polymer, 2001, 42, 9015-9023.	3.8	105
110	Nature of Strain-Induced Structures in Natural and Synthetic Rubbers under Stretching. Macromolecules, 2003, 36, 5915-5917.	4.8	104
111	In vitro non-viral gene delivery with nanofibrous scaffolds. Nucleic Acids Research, 2005, 33, e170-e170.	14.5	102
112	Thermal Stability of Shear-Induced Shish-Kebab Precursor Structure from High Molecular Weight Polyethylene Chains. Macromolecules, 2006, 39, 2209-2218.	4.8	102
113	Super-Robust Polylactide Barrier Films by Building Densely Oriented Lamellae Incorporated with Ductile in Situ Nanofibrils of Poly(butylene adipate- <i>co</i> -terephthalate). ACS Applied Materials & Interfaces, 2016, 8, 8096-8109.	8.0	102
114	Crystallization-Induced Undulated Morphology in Polystyrene-b-Poly(l-lactide) Block Copolymer. Macromolecules, 2004, 37, 5985-5994.	4.8	99
115	Debranching and crystallization of waxy maize starch in relation to enzyme digestibility. Carbohydrate Polymers, 2010, 81, 385-393.	10.2	99
116	Fabrication of thin-film nanofibrous composite membranes by interfacial polymerization using ionic liquids as additives. Journal of Membrane Science, 2010, 365, 52-58.	8.2	98
117	Hierarchical Assembly of a Series of Rodâ^'Coil Block Copolymers:Â Supramolecular LC Phase in Nanoenviroment. Macromolecules, 2004, 37, 2854-2860.	4.8	97
118	Structure Development during the Melt Spinning of Polyethylene and Poly(vinylidene fluoride) Fibers by in Situ Synchrotron Small- and Wide-Angle X-ray Scattering Techniques. Macromolecules, 1999, 32, 8121-8132.	4.8	96
119	Crystallization and Stress Relaxation in Highly Stretched Samples of Natural Rubber and Its Synthetic Analogue. Macromolecules, 2006, 39, 5100-5105.	4.8	95
120	Shear Flow and Carbon Nanotubes Synergistically Induced Nonisothermal Crystallization of Poly(lactic acid) and Its Application in Injection Molding. Biomacromolecules, 2012, 13, 3858-3867.	5.4	95
121	Strainâ€induced crystallization and mechanical properties of functionalized graphene sheetâ€filled natural rubber. Journal of Polymer Science, Part B: Polymer Physics, 2012, 50, 718-723.	2.1	94
122	Poly(ethyleneimine) nanofibrous affinity membrane fabricated via one step wet-electrospinning from poly(vinyl alcohol)-doped poly(ethyleneimine) solution system and its application. Journal of Membrane Science, 2011, 379, 191-199.	8.2	93
123	Efficient Removal of Arsenic Using Zinc Oxide Nanocrystal-Decorated Regenerated Microfibrillated Cellulose Scaffolds. ACS Sustainable Chemistry and Engineering, 2019, 7, 6140-6151.	6.7	93
124	Understanding the Mechanistic Behavior of Highly Charged Cellulose Nanofibers in Aqueous Systems. Macromolecules, 2018, 51, 1498-1506.	4.8	92
125	UV-cured poly(vinyl alcohol) ultrafiltration nanofibrous membrane based on electrospun nanofiber scaffolds. Journal of Membrane Science, 2009, 328, 1-5.	8.2	91
126	Nanotailored Crystalline Morphology in Hexagonally Perforated Layers of a Self-Assembled PS-b-PEO Diblock Copolymer. Macromolecules, 2002, 35, 3553-3562.	4.8	90

#	Article	IF	CITATIONS
127	Novel nanofibrous scaffolds for water filtration with bacteria and virus removal capability. Journal of Electron Microscopy, 2011, 60, 201-209.	0.9	90
128	Effect of Network-Chain Length on Strain-Induced Crystallization of NR and IR Vulcanizates. Rubber Chemistry and Technology, 2004, 77, 711-723.	1.2	89
129	Effects of high molecular weight species on shear-induced orientation and crystallization of isotactic polypropylene. Polymer, 2006, 47, 5657-5668.	3.8	89
130	In Situ Synchrotron X-ray Scattering Study on Isotactic Polypropylene Crystallization under the Coexistence of Shear Flow and Carbon Nanotubes. Macromolecules, 2011, 44, 8080-8092.	4.8	89
131	Strong Shear Flow-Driven Simultaneous Formation of Classic Shish-Kebab, Hybrid Shish-Kebab, and Transcrystallinity in Poly(lactic acid)/Natural Fiber Biocomposites. ACS Sustainable Chemistry and Engineering, 2013, 1, 1619-1629.	6.7	89
132	Strain-Induced Crystallization of Natural Rubber: Effect of Proteins and Phospholipids. Rubber Chemistry and Technology, 2008, 81, 753-766.	1.2	88
133	Highly efficient and sustainable carboxylated cellulose filters for removal of cationic dyes/heavy metals ions. Chemical Engineering Journal, 2020, 389, 123458.	12.7	88
134	Comparison of poly(ethylene oxide) crystal orientations and crystallization behaviors in nano-confined cylinders constructed by a poly(ethylene oxide)-b-polystyrene diblock copolymer and a blend of poly(ethylene oxide)-b-polystyrene and polystyrene. Polymer, 2006, 47, 5457-5466.	3.8	87
135	Enhanced Mechanical Performance of Selfâ€Bundled Electrospun Fiber Yarns via Postâ€Treatments. Macromolecular Rapid Communications, 2008, 29, 826-831.	3.9	87
136	Isothermal thickening and thinning processes in low-molecular-weight poly(ethylene oxide) fractions crystallized from the melt. 4. End-group dependence. Macromolecules, 1993, 26, 5105-5117.	4.8	85
137	Probing the Nature of Strain-Induced Crystallization in Polyisoprene Rubber by Combined Thermomechanical and In Situ X-ray Diffraction Techniques. Macromolecules, 2005, 38, 7064-7073.	4.8	85
138	Design and fabrication of electrospun polyethersulfone nanofibrous scaffold for highâ€flux nanofiltration membranes. Journal of Polymer Science, Part B: Polymer Physics, 2009, 47, 2288-2300.	2.1	84
139	Thin-film nanofibrous composite membranes containing cellulose or chitin barrier layers fabricated by ionic liquids. Polymer, 2011, 52, 2594-2599.	3.8	84
140	High flux ethanol dehydration using nanofibrous membranes containing graphene oxide barrier layers. Journal of Materials Chemistry A, 2013, 1, 12998.	10.3	84
141	Self-roughened omniphobic coatings on nanofibrous membrane for membrane distillation. Separation and Purification Technology, 2018, 206, 14-25.	7.9	82
142	Nanocellulose for Sustainable Water Purification. Chemical Reviews, 2022, 122, 8936-9031.	47.7	82
143	Strain-Induced Molecular Orientation and Crystallization in Natural and Synthetic Rubbers under Uniaxial Deformation by In-situ Synchrotron X-ray Study. Rubber Chemistry and Technology, 2004, 77, 317-335.	1.2	81
144	Structural formation of amorphous poly(ethylene terephthalate) during uniaxial deformation above glass temperature. Polymer, 2004, 45, 905-918.	3.8	81

#	Article	IF	CITATIONS
145	Nanofibrous ultrafiltration membranes containing cross-linked poly(ethylene glycol) and cellulose nanofiber composite barrier layer. Polymer, 2014, 55, 366-372.	3.8	80
146	Nanofiltration membranes based on thin-film nanofibrous composites. Journal of Membrane Science, 2014, 469, 188-197.	8.2	80
147	Phase Diagram of a Nearly Isorefractive Polyolefin Blend. Macromolecules, 2002, 35, 1072-1078.	4.8	79
148	Crystallization and structure formation of poly(l-lactide-co-meso-lactide) random copolymers: a time-resolved wide- and small-angle X-ray scattering study. Polymer, 2003, 44, 711-717.	3.8	79
149	Efficient Removal of UO ₂ ²⁺ from Water Using Carboxycellulose Nanofibers Prepared by the Nitro-Oxidation Method. Industrial & Engineering Chemistry Research, 2017, 56, 13885-13893.	3.7	79
150	Single Molecular Layer of Silk Nanoribbon as Potential Basic Building Block of Silk Materials. ACS Nano, 2018, 12, 11860-11870.	14.6	79
151	Lateral Packing of Mineral Crystals in Bone Collagen Fibrils. Biophysical Journal, 2008, 95, 1985-1992.	0.5	77
152	Interfacial Shish-Kebabs Lengthened by Coupling Effect of In Situ Flexible Nanofibrils and Intense Shear Flow: Achieving Hierarchy To Conquer the Conflicts between Strength and Toughness of Polylactide. ACS Applied Materials & Interfaces, 2017, 9, 10148-10159.	8.0	77
153	Comparison of crystallization kinetics in various nanoconfined geometries. Polymer, 2004, 45, 2931-2939.	3.8	76
154	The effects of endlinking network and entanglement to stress–strain relation and strain-induced crystallization of un-vulcanized and vulcanized natural rubber. Polymer, 2012, 53, 3325-3330.	3.8	76
155	Synthesis and Characterization of Segmented Polyurethanes Containing Polyhedral Oligomeric Silsesquioxanes Nanostructured Molecules. High Performance Polymers, 2000, 12, 565-571.	1.8	74
156	Eco-friendly poly(acrylic acid)-sodium alginate nanofibrous hydrogel: A multifunctional platform for superior removal of Cu(II) and sustainable catalytic applications. Colloids and Surfaces A: Physicochemical and Engineering Aspects, 2018, 558, 228-241.	4.7	74
157	An <i>in Situ</i> X-ray Structural Study of Olefin Block and Random Copolymers under Uniaxial Deformation. Macromolecules, 2010, 43, 1922-1929.	4.8	73
158	Anionic Surfactant-Triggered Steiner Geometrical Poly(vinylidene fluoride) Nanofiber/Nanonet Air Filter for Efficient Particulate Matter Removal. ACS Applied Materials & Interfaces, 2018, 10, 42891-42904.	8.0	73
159	Novel image analysis of two-dimensional X-ray fiber diffraction patterns: example of a polypropylene fiber drawing study. Journal of Applied Crystallography, 2000, 33, 1031-1036.	4.5	72
160	Highly permeable nanofibrous composite microfiltration membranes for removal of nanoparticles and heavy metal ions. Separation and Purification Technology, 2020, 233, 115976.	7.9	72
161	Mechanism of Structural Formation by Uniaxial Deformation in Amorphous Poly(ethylene) Tj ETQq1 1 0.784314	⊦rg₿T,/Ove 4.8	erlock 10 Tf 50
162	In-Situ X-ray Scattering Studies of a Unique Toughening Mechanism in Surface-Modified Carbon	4.8	70

Nanofiber/ÚHMWPE Nanocomposite Films. Macromolecules, 2005, 38, 3883-3893.

#	Article	IF	CITATIONS
163	High flux low pressure thin film nanocomposite ultrafiltration membranes based on nanofibrous substrates. Separation and Purification Technology, 2013, 108, 143-151.	7.9	70
164	Silver Nanoparticle-Enabled Photothermal Nanofibrous Membrane for Light-Driven Membrane Distillation. Industrial & Engineering Chemistry Research, 2019, 58, 3269-3281.	3.7	70
165	Polymorphism in poly(aryl ether ketone)s. Polymer, 1994, 35, 2290-2295.	3.8	69
166	SAXS studies of lamellar level morphological changes during crystallization and melting in PEEK. Polymer, 1996, 37, 5357-5365.	3.8	69
167	Thiol-functionalized chitin nanofibers for As (III) adsorption. Polymer, 2015, 60, 9-17.	3.8	69
168	Superior Impact Toughness and Excellent Storage Modulus of Poly(lactic acid) Foams Reinforced by Shish-Kebab Nanoporous Structure. ACS Applied Materials & Interfaces, 2017, 9, 21071-21076.	8.0	69
169	Thin-film nanofibrous composite reverse osmosis membranes for desalination. Desalination, 2017, 420, 91-98.	8.2	69
170	Lead removal from water using carboxycellulose nanofibers prepared by nitro-oxidation method. Cellulose, 2018, 25, 1961-1973.	4.9	69
171	Effects of molecular weight on poly(ω-pentadecalactone) mechanical and thermal properties. Polymer, 2010, 51, 1088-1099.	3.8	67
172	From Nanofibrillar to Nanolaminar Poly(butylene succinate): Paving the Way to Robust Barrier and Mechanical Properties for Full-Biodegradable Poly(lactic acid) Films. ACS Applied Materials & Interfaces, 2015, 7, 8023-8032.	8.0	67
173	Integrated polyamide thin-film nanofibrous composite membrane regulated by functionalized interlayer for efficient water/isopropanol separation. Journal of Membrane Science, 2018, 553, 70-81.	8.2	67
174	Crystallization Behavior of Poly(ethylene oxide) and Its Blends Using Time-Resolved Wide- and Small-Angle X-ray Scattering. Macromolecules, 2000, 33, 4842-4849.	4.8	66
175	Structure Changes during Uniaxial Deformation of Ethylene-Based Semicrystalline Ethyleneâ^Propylene Copolymer. 1. SAXS Study. Macromolecules, 2003, 36, 1920-1929.	4.8	66
176	Tuning the Superstructure of Ultrahigh-Molecular-Weight Polyethylene/Low-Molecular-Weight Polyethylene Blend for Artificial Joint Application. ACS Applied Materials & Interfaces, 2012, 4, 1521-1529.	8.0	66
177	Arsenic(III) Removal by Nanostructured Dialdehyde Cellulose–Cysteine Microscale and Nanoscale Fibers. ACS Omega, 2019, 4, 22008-22020.	3.5	66
178	Crystal Orientation Change and Its Origin in One-Dimensional Nanoconfinement Constructed by Polystyrene- <i>block</i> -poly(ethylene oxide) Single Crystal Mats. Macromolecules, 2008, 41, 8114-8123.	4.8	65
179	Interactions between Crystalline and Amorphous Domains in Semicrystalline Polymers:Â Small-Angle X-ray Scattering Studies of the Brill Transition in Nylon 6,6. Macromolecules, 1999, 32, 5594-5599.	4.8	64
180	On the nature of multiple melting in poly(ethylene terephthalate) (PET) and its copolymers with cyclohexylene dimethylene terephthalate (PET/CT). Polymer, 2003, 44, 1527-1535.	3.8	64

#	Article	IF	CITATIONS
181	Crystal Morphology and Phase Identifications in Poly(aryl ether ketone)s and Their Copolymers. 1. Polymorphism in PEKK. Macromolecules, 1994, 27, 2136-2140.	4.8	63
182	Dislocation-Controlled Perforated Layer Phase in a PEO- b-PS Diblock Copolymer. Physical Review Letters, 2001, 86, 6030-6033.	7.8	63
183	Shear-induced crystallization in isotactic polypropylene containing ultra-high molecular weight polyethylene oriented precursor domains. Polymer, 2005, 46, 3096-3104.	3.8	62
184	Shear-induced crystallization of isotactic polypropylene within the oriented scaffold of noncrystalline ultrahigh molecular weight polyethylene. Polymer, 2005, 46, 8859-8871.	3.8	62
185	Structure Evolution during Cyclic Deformation of an Elastic Propylene-Based Ethyleneâ^'Propylene Copolymer. Macromolecules, 2006, 39, 3588-3597.	4.8	62
186	Functionalization of poly(L-lactide) nanofibrous scaffolds with bioactive collagen molecules. Journal of Biomedical Materials Research - Part A, 2007, 83A, 1117-1127.	4.0	62
187	Low pressure UV-cured CS–PEO–PTEGDMA/PAN thin film nanofibrous composite nanofiltration membranes for anionic dye separation. Journal of Materials Chemistry A, 2016, 4, 15575-15588.	10.3	62
188	Effect of the heterogeneous distribution of lamellar stacks on amorphous relaxations in semicrystalline polymers. Polymer, 1995, 36, 2553-2558.	3.8	61
189	Structural developments in synthetic rubbers during uniaxial deformation byin situ synchrotron X-ray diffraction. Journal of Polymer Science, Part B: Polymer Physics, 2004, 42, 956-964.	2.1	61
190	Superstructure Evolution in Poly(ethylene terephthalate) during Uniaxial Deformation above Glass Transition Temperature. Macromolecules, 2006, 39, 2909-2920.	4.8	61
191	Real-Time Crystallization of Organoclay Nanoparticle Filled Natural Rubber under Stretching. Macromolecules, 2008, 41, 2295-2298.	4.8	61
192	Low pressure high flux thin film nanofibrous composite membranes prepared by electrospraying technique combined with solution treatment. Journal of Membrane Science, 2012, 394-395, 241-247.	8.2	61
193	Strong and tough micro/nanostructured poly(lactic acid) by mimicking the multifunctional hierarchy of shell. Materials Horizons, 2014, 1, 546-552.	12.2	61
194	Relationships between Structure and Rheology in Model Nanocomposites of Ethyleneâ^'Vinyl-Based Copolymers and Organoclays. Macromolecules, 2005, 38, 3765-3775.	4.8	60
195	Easy alignment and effective nucleation activity of ramie fibers in injectionâ€molded poly(lactic acid) biocomposites. Biopolymers, 2012, 97, 825-839.	2.4	60
196	Molecular dynamics and microstructure development during cold crystallization in poly(ether-ether-ketone) as revealed by real time dielectric and x-ray methods. Journal of Chemical Physics, 2001, 115, 3804-3813.	3.0	59
197	Probing nucleation and growth behavior of twisted kebabs from shish scaffold in sheared polyethylene melts by in situ X-ray studies. Polymer, 2007, 48, 4511-4519.	3.8	59
198	Multiâ€scaled microstructures in natural rubber characterized by synchrotron Xâ€ray scattering and optical microscopy. Journal of Polymer Science, Part B: Polymer Physics, 2008, 46, 2456-2464.	2.1	59

#	Article	IF	CITATIONS
199	Chemical crosslinking and biophysical properties of electrospun hyaluronic acid based ultra-thin fibrous membranes. Polymer, 2009, 50, 3762-3769.	3.8	59
200	Crystal and Crystallites Structure of Natural Rubber and Synthetic <i>cis</i> -1,4-Polyisoprene by a New Two Dimensional Wide Angle X-ray Diffraction Simulation Method. I. Strain-Induced Crystallization. Macromolecules, 2013, 46, 4520-4528.	4.8	59
201	Structure characterization of cellulose nanofiber hydrogel as functions of concentration and ionic strength. Cellulose, 2017, 24, 5417-5429.	4.9	59
202	New Insight of Isothermal Melt Crystallization in Poly(aryl ether ether ketone) via Time-Resolved Simultaneous Small-Angle X-ray Scattering/Wide-Angle X-ray Diffraction Measurements. Macromolecules, 1995, 28, 6931-6936.	4.8	58
203	"Plastic Deformation―Mechanism and Phase Transformation in a Shear-Induced Metastable Hexagonally Perforated Layer Phase of a Polystyrene-b-poly(ethylene oxide) Diblock Copolymer. Macromolecules, 2003, 36, 3180-3188.	4.8	58
204	New Insights into Lamellar Structure Development and SAXS/WAXD Sequence Appearance during Uniaxial Stretching of Amorphous Poly(ethylene terephthalate) above Glass Transition Temperature. Macromolecules, 2008, 41, 2859-2867.	4.8	58
205	Cationic Dialdehyde Nanocellulose from Sugarcane Bagasse for Efficient Chromium(VI) Removal. ACS Sustainable Chemistry and Engineering, 2020, 8, 4734-4744.	6.7	58
206	Role of Stably Entangled Chain Network Density in Shish-Kebab Formation in Polyethylene under an Intense Flow Field. Macromolecules, 2015, 48, 6652-6661.	4.8	57
207	Combined effect of shear and fibrous fillers on orientation-induced crystallization in discontinuous aramid fiber/isotactic polypropylene composites. Polymer, 2008, 49, 295-302.	3.8	56
208	Rheological study of carbon nanofiber induced physical gelation in polyolefin nanocomposite melt. Polymer, 2005, 46, 11591-11599.	3.8	55
209	Effects of Block Architecture on Structure and Mechanical Properties of Olefin Block Copolymers under Uniaxial Deformation. Macromolecules, 2011, 44, 3670-3673.	4.8	55
210	Isothermal crystallization kinetics of poly(ether ketone ketone) and its carbon-fibre-reinforced composites. Polymer, 1991, 32, 2799-2805.	3.8	54
211	Structure development in the early stages of crystallization during melt spinning. Polymer, 2002, 43, 1873-1875.	3.8	54
212	Ultra-fine electrospun nanofibrous membranes for multicomponent wastewater treatment: Filtration and Purification Technology, 2020, 242, 116794.	7.9	53
213	Super-hydrophobic modification of porous natural polymer "luffa sponge―for oil absorption. Polymer, 2017, 126, 470-476.	3.8	52
214	Robust superhydrophobic dual layer nanofibrous composite membranes with a hierarchically structured amorphous polypropylene skin for membrane distillation. Journal of Materials Chemistry A, 2019, 7, 11282-11297.	10.3	52
215	A laserâ€∎ided prealigned pinhole collimator for synchrotron x rays. Review of Scientific Instruments, 1994, 65, 597-602.	1.3	51
216	Structure development during melt spinning and subsequent annealing of polybutene-1 fibers. Journal of Polymer Science, Part B: Polymer Physics, 2000, 38, 1872-1882.	2.1	49

#	Article	IF	CITATIONS
217	Characterization of TEMPO-oxidized cellulose nanofibers in aqueous suspension by small-angle X-ray scattering. Journal of Applied Crystallography, 2014, 47, 788-798.	4.5	49
218	High filtration performance thin film nanofibrous composite membrane prepared by electrospraying technique and hot-pressing treatment. Journal of Membrane Science, 2016, 499, 470-479.	8.2	49
219	Structure and property studies of bioabsorbable poly(glycolide-co-lactide) fiber during processing and in vitro degradation. Polymer, 2002, 43, 5527-5534.	3.8	48
220	Exploring the Nature of Cellulose Microfibrils. Biomacromolecules, 2015, 16, 1201-1209.	5.4	48
221	Nature of Shear-Induced Primary Nuclei in iPP Melt. Journal of Macromolecular Science - Physics, 2003, 42, 515-531.	1.0	47
222	Deformation-induced highly oriented and stable mesomorphic phase in quenched isotactic polypropylene. Polymer, 2007, 48, 6934-6947.	3.8	47
223	Thin-Film Nanofibrous Composite Ultrafiltration Membranes Based on Polyvinyl Alcohol Barrier Layer Containing Directional Water Channels. Industrial & Engineering Chemistry Research, 2010, 49, 11978-11984.	3.7	47
224	Molecular dynamics of natural rubber as revealed by dielectric spectroscopy: The role of natural cross–linking. Soft Matter, 2010, 6, 3636.	2.7	47
225	High Aspect Ratio Carboxycellulose Nanofibers Prepared by Nitro-Oxidation Method and Their Nanopaper Properties. ACS Applied Nano Materials, 2018, 1, 3969-3980.	5.0	47
226	Morphological features and melting behavior of nanocomposites based on isotactic polypropylene and multiwalled carbon nanotubes. Journal of Applied Polymer Science, 2007, 106, 2640-2647.	2.6	46
227	Role of stearic acid in the strain-induced crystallization of crosslinked natural rubber and synthetic cis-1,4-polyisoprene. Polymer, 2007, 48, 3801-3808.	3.8	46
228	The relationship between microstructure and toughness of biaxially oriented semicrystalline polyester films. Polymer, 2008, 49, 2507-2514.	3.8	46
229	Molecular orientation and stress relaxation during strain-induced crystallization of vulcanized natural rubber. Polymer Journal, 2010, 42, 474-481.	2.7	46
230	Real-Time Structure Changes during Uniaxial Stretching of Poly(ω-pentadecalactone) by <i>in Situ</i> Synchrotron WAXD/SAXS Techniques. Macromolecules, 2011, 44, 3874-3883.	4.8	46
231	Antifouling nanocellulose membranes: How subtle adjustment of surface charge lead to self-cleaning property. Journal of Membrane Science, 2021, 618, 118739.	8.2	46
232	Uniaxial deformation of an elastomer nanocomposite containing modified carbon nanofibers by in situ synchrotron X-ray diffraction. Polymer, 2005, 46, 5103-5117.	3.8	45
233	The role of polymers in breakthrough technologies for water purification. Journal of Polymer Science, Part B: Polymer Physics, 2009, 47, 2431-2435.	2.1	45
234	Crystal and Crystallites Structure of Natural Rubber and Peroxide-Vulcanized Natural Rubber by a Two-Dimensional Wide-Angle X-ray Diffraction Simulation Method. II. Strain-Induced Crystallization versus Temperature-Induced Crystallization. Macromolecules, 2013, 46, 9712-9721.	4.8	45

#	Article	IF	CITATIONS
235	Cross-Sections of Nanocellulose from Wood Analyzed by Quantized Polydispersity of Elementary Microfibrils. ACS Nano, 2020, 14, 16743-16754.	14.6	45
236	Electrospun Nanofibrous Scaffolds for Biomedical Applications. Journal of Biomedical Nanotechnology, 2005, 1, 115-132.	1.1	44
237	Suppressing the Skin–Core Structure of Injection-Molded Isotactic Polypropylene via Combination of an in situ Microfibrillar Network and an Interfacial Compatibilizer. Journal of Physical Chemistry B, 2011, 115, 7497-7504.	2.6	44
238	Continuous fabrication of cellulose nanocrystal/poly(ethylene glycol) diacrylate hydrogel fiber from nanocomposite dispersion: Rheology, preparation and characterization. Polymer, 2017, 123, 55-64.	3.8	44
239	In Vitro Mineralization of Collagen in Demineralized Fish Bone. Macromolecular Chemistry and Physics, 2005, 206, 43-51.	2.2	43
240	Shear-Induced Precursor Relaxation-Dependent Growth Dynamics and Lamellar Orientation of β-Crystals in β-Nucleated Isotactic Polypropylene. Journal of Physical Chemistry B, 2015, 119, 5716-5727.	2.6	43
241	In Situ Nanofibrillar Networks Composed of Densely Oriented Polylactide Crystals as Efficient Reinforcement and Promising Barrier Wall for Fully Biodegradable Poly(butylene succinate) Composite Films. ACS Sustainable Chemistry and Engineering, 2016, 4, 2887-2897.	6.7	43
242	Novel thin-film nanofibrous composite membranes containing directional toxin transport nanochannels for efficient and safe hemodialysis application. Journal of Membrane Science, 2019, 582, 151-163.	8.2	43
243	Elucidating the Opportunities and Challenges for Nanocellulose Spinning. Advanced Materials, 2021, 33, e2001238.	21.0	43
244	Facile synthesis of TiO2/CNC nanocomposites for enhanced Cr(VI) photoreduction: Synergistic roles of cellulose nanocrystals. Carbohydrate Polymers, 2020, 233, 115838.	10.2	43
245	Preferred Orientation in Polymer Fiber Scattering. Polymer Reviews, 2010, 50, 91-111.	10.9	42
246	2D WAXS/SAXS study on isotactic propylene-1-butylene random copolymer subjected to uniaxial stretching: The influence of temperature. Polymer, 2013, 54, 1432-1439.	3.8	42
247	Strong Silk Fibers Containing Cellulose Nanofibers Generated by a Bioinspired Microfluidic Chip. ACS Sustainable Chemistry and Engineering, 2019, 7, 14765-14774.	6.7	42
248	Synthesis and Characterization of Poly(oxy-1,3-phenylenecarbonyl-1,4-phenylene) and Related Polymers. Macromolecules, 1996, 29, 6432-6441.	4.8	41
249	Isothermal Thickening and Thinning Processes in Low-Molecular-Weight Poly(ethylene oxide) Fractions Crystallized from the Melt. 8. Molecular Shape Dependence§. Macromolecules, 1999, 32, 4784-4793.	4.8	41
250	In situ observation of low molecular weight poly(ethylene oxide) crystal melting, recrystallization. Polymer, 2003, 44, 6051-6058.	3.8	41
251	Tough and Elastic Thermoplastic Organogels and Elastomers Made of Semicrystalline Polyolefin-Based Block Copolymers. Macromolecules, 2012, 45, 5604-5618.	4.8	41
252	Engineering construction of robust superhydrophobic two-tier composite membrane with interlocked structure for membrane distillation. Journal of Membrane Science, 2020, 598, 117813.	8.2	41

#	Article	IF	CITATIONS
253	Biodegradable silk fibroin-based bio-piezoelectric/triboelectric nanogenerators as self-powered electronic devices. Nano Energy, 2022, 96, 107101.	16.0	41
254	Lamellar Formation and Relaxation in Simple Sheared Poly(ethylene terephthalate) by Small-Angle X-ray Scattering. Macromolecules, 2006, 39, 2930-2939.	4.8	40
255	In-Situ X-ray Deformation Study of Fluorinated Multiwalled Carbon Nanotube and Fluorinated Ethyleneâ^'Propylene Nanocomposite Fibers. Macromolecules, 2006, 39, 5427-5437.	4.8	40
256	Biofouling-resistant nanocellulose layer in hierarchical polymeric membranes: Synthesis, characterization and performance. Journal of Membrane Science, 2019, 579, 162-171.	8.2	40
257	Side-Chain Liquid Crystalline Poly(meth)acrylates with Bent-Core Mesogens. Macromolecules, 2007, 40, 840-848.	4.8	39
258	A durable thin-film nanofibrous composite nanofiltration membrane prepared by interfacial polymerization on a double-layer nanofibrous scaffold. RSC Advances, 2017, 7, 18001-18013.	3.6	39
259	Isothermal Thickening and Thinning Processes in Low Molecular Weight Poly(ethylene oxide) Fractions Crystallized from the Melt. 5. Effect of Chain Defects. Macromolecules, 1996, 29, 8816-8823.	4.8	38
260	Processingâ€structureâ€mechanical property relationships of semicrystalline polyolefinâ€based block copolymers. Journal of Polymer Science, Part B: Polymer Physics, 2010, 48, 1428-1437.	2.1	38
261	Design and Synthesis of Network-Forming Triblock Copolymers Using Tapered Block Interfaces. ACS Macro Letters, 2012, 1, 519-523.	4.8	38
262	Plastic Deformation of Semicrystalline Polyethylene by X-ray Scattering: Comparison with Atomistic Simulations. Macromolecules, 2013, 46, 5279-5289.	4.8	38
263	Simultaneous improvement of strength and toughness in fiber reinforced isotactic polypropylene composites by shear flow and a l ² -nucleating agent. RSC Advances, 2014, 4, 14766-14776.	3.6	38
264	Crystalline Homopolyimides and Copolyimides Derived from 3,3',4,4'-Biphenyltetracarboxylic Dianhydride/1,3-Bis(4-aminophenoxy)benzene/1,12-Dodecanediamine. 1. Materials, Preparation, and Characterization. Macromolecules, 1995, 28, 6926-6930.	4.8	37
265	Step-Cycle Mechanical Processing of Gels of sPP- <i>b</i> -EPR- <i>b</i> -sPP Triblock Copolymer in Mineral Oil. Macromolecules, 2010, 43, 6782-6788.	4.8	37
266	Phase Transitions in Prequenched Mesomorphic Isotactic Polypropylene during Heating and Annealing Processes As Revealed by Simultaneous Synchrotron SAXS and WAXD Technique. Journal of Physical Chemistry B, 2012, 116, 147-153.	2.6	37
267	Dynamic Study of Crystallization- and Melting-Induced Phase Separation in PEEK/PEKK Blends. Macromolecules, 1997, 30, 4544-4550.	4.8	36
268	Poly(ethylene oxide) Crystal Orientation Changes in an Inverse Hexagonal Cylindrical Phase Morphology Constructed by a Poly(ethylene oxide)-block-polystyrene Diblock Copolymer. Macromolecules, 2007, 40, 526-534.	4.8	36
269	Chain Dynamics and Strain-Induced Crystallization of Pre- and Postvulcanized Natural Rubber Latex Using Proton Multiple Quantum NMR and Uniaxial Deformation by <i>in Situ</i> Synchrotron X-ray Diffraction. Macromolecules, 2012, 45, 6491-6503.	4.8	36
270	Carbon nanotube surface-induced crystallization of polyethylene terephthalate (PET). Polymer, 2014, 55, 642-650.	3.8	36

#	Article	IF	CITATIONS
271	Improvement of meltdown temperature of lithium-ion battery separator using electrospun polyethersulfone membranes. Polymer, 2016, 107, 163-169.	3.8	36
272	Integrated dynamic wet spinning of core-sheath hydrogel fibers for optical-to-brain/tissue communications. National Science Review, 2021, 8, nwaa209.	9.5	36
273	Crystalline Homopolyimides and Copolyimides Derived from 3,3â€,4,4â€-Biphenyltetracarboxylic Dianhydride/1,3-Bis(4-aminophenoxy)benzene/1,12-Dodecanediamine. 2. Crystallization, Melting, and Morphology. Macromolecules, 1996, 29, 135-142.	4.8	35
274	In-Situ Synchrotron WAXD/SAXS Studies of Structural Development during PBO/PPA Solution Spinning. Macromolecules, 2002, 35, 433-439.	4.8	35
275	Self-reinforced polyethylene blend for artificial joint application. Journal of Materials Chemistry B, 2014, 2, 971.	5.8	35
276	Insight into unique deformation behavior of oriented isotactic polypropylene with branched shish-kebabs. Polymer, 2015, 60, 274-283.	3.8	35
277	A.C. dielectric and TSC studies of constrained amorphous motions in flexible polymers including poly(oxymethylene) and miscible blends. Journal of Polymer Science, Part B: Polymer Physics, 1997, 35, 2121-2132.	2.1	33
278	DETERMINATION OF CRYSTALLINE LAMELLAR THICKNESS IN POLY(ETHYLENE TEREPHTHALATE) USING SMALL-ANGLE X-RAY SCATTERING AND TRANSMISSION ELECTRON MICROSCOPY*. Journal of Macromolecular Science - Physics, 2001, 40, 625-638.	1.0	33
279	Crystallization of Polystyrene-block-[Syndiotactic Poly(propylene)] Block Copolymers from Confinement to Breakout. Macromolecular Rapid Communications, 2005, 26, 107-111.	3.9	33
280	Large Scale Production of Continuous Hydrogel Fibers with Anisotropic Swelling Behavior by Dynamic rosslinking‧pinning. Macromolecular Rapid Communications, 2016, 37, 1795-1801.	3.9	33
281	Enhanced pervaporation performance of polyamide membrane with synergistic effect of porous nanofibrous support and trace graphene oxide lamellae. Chemical Engineering Science, 2019, 196, 265-276.	3.8	33
282	Crystal Structure, Morphology, and Phase Transitions in Aromatic Polyimide Oligomers. 1. Poly(4,4'-oxydiphenylene pyromellitimide). Macromolecules, 1994, 27, 989-996.	4.8	32
283	Competition between liquid crystallinity and block copolymerself-assembly in core–shell rod–coil block copolymers. Soft Matter, 2008, 4, 458-461.	2.7	32
284	Phase Behavior of Neat Triblock Copolymers and Copolymer/Homopolymer Blends Near Network Phase Windows. Macromolecules, 2010, 43, 9039-9048.	4.8	32
285	Time-Resolved Synchrotron X-ray Scattering Study on Propylene–1-Butylene Random Copolymer Subjected to Uniaxial Stretching at High Temperatures. Macromolecules, 2012, 45, 951-961.	4.8	32
286	Effects of degumming conditions on electro-spinning rate of regenerated silk. International Journal of Biological Macromolecules, 2013, 61, 50-57.	7.5	32
287	Crystallization study of a thermoplastic polyimide (new-TPI). Journal of Polymer Science, Part B: Polymer Physics, 1994, 32, 737-747.	2.1	31
288	Morphology development during isothermal crystallization. I. Isotactic and atactic polypropylene blends. Journal of Polymer Science, Part B: Polymer Physics, 2000, 38, 2580-2590.	2.1	31

#	Article	IF	CITATIONS
289	Title is missing!. Journal of Materials Science, 2001, 36, 3071-3077.	3.7	31
290	Shearâ€Induced Orientation and Structure Development in Isotactic Polypropylene Melt Containing Modified Carbon Nanofibers. Journal of Macromolecular Science - Physics, 2006, 45, 247-261.	1.0	31
291	Small-angle X-ray scattering study of intramuscular fish bone: collagen fibril superstructure determined from equidistant meridional reflections. Journal of Applied Crystallography, 2008, 41, 252-261.	4.5	31
292	A Springâ€Like Behavior of Chiral Block Copolymer with Helical Nanostructure Driven by Crystallization. Advanced Functional Materials, 2009, 19, 448-459.	14.9	31
293	Polypentadecalactone prepared by lipase catalysis: crystallization kinetics and morphology. Polymer International, 2009, 58, 944-953.	3.1	31
294	Characterization of nanoclay orientation in polymer nanocomposite film by small-angle X-ray scattering. Polymer, 2010, 51, 5255-5266.	3.8	31
295	Crystallization of poly(aryl ether ketone ketone) copolymers containing terephthalate/isophthalate moieties. Journal of Polymer Science, Part B: Polymer Physics, 1994, 32, 2585-2594.	2.1	30
296	Structure and morphology development in syndiotactic polypropylene during isothermal crystallization and subsequent melting. Journal of Polymer Science, Part B: Polymer Physics, 2001, 39, 2982-2995.	2.1	30
297	Pathway-Dependent Melting in a Low-Molecular-Weight Polyethylene-block-Poly(ethylene oxide) Diblock Copolymer. Macromolecular Rapid Communications, 2004, 25, 853-857.	3.9	30
298	Thermal stability of shear-induced precursor structures in isotactic polypropylene by rheo-X-ray techniques with couette flow geometry. Journal of Polymer Science, Part B: Polymer Physics, 2006, 44, 3553-3570.	2.1	30
299	Surface Modification of Nanoclays by Catalytically Active Transition Metal Ions. Langmuir, 2007, 23, 9808-9815.	3.5	30
300	An in-situ X-ray scattering study during uniaxial stretching of ionic liquid/ultra-high molecular weight polyethylene blends. Polymer, 2011, 52, 4610-4618.	3.8	30
301	Micro-nano structure nanofibrous p-sulfonatocalix[8]arene complex membranes for highly efficient and selective adsorption of lanthanum(<scp>iii</scp>) ions in aqueous solution. RSC Advances, 2015, 5, 21178-21188.	3.6	30
302	Rice husk based nanocellulose scaffolds for highly efficient removal of heavy metal ions from contaminated water. Environmental Science: Water Research and Technology, 2020, 6, 3080-3090.	2.4	30
303	Effect of miscible polymer diluents on the development of lamellar morphology in poly(oxymethylene) blends. Journal of Polymer Science, Part B: Polymer Physics, 1999, 37, 3115-3122.	2.1	29
304	Manipulating the microstructure and rheology in polymer-organoclay composites. Polymer Engineering and Science, 2002, 42, 1841-1851.	3.1	29
305	Probing Flow-Induced Precursor Structures in Blown Polyethylene Films by Synchrotron X-rays during Constrained Melting. Macromolecules, 2005, 38, 5128-5136.	4.8	29
306	Stabilizing Thin Film Polymer Bilayers against Dewetting Using Multiwalled Carbon Nanotubes. Macromolecules, 2007, 40, 9510-9516.	4.8	29

#	ARTICLE	IF	CITATIONS
307	Ultra-strong, tough and high wear resistance high-density polyethylene for structural engineering application: A facile strategy towards using the combination of extensional dynamic oscillatory shear flow and ultra-high-molecular-weight polyethylene. Composites Science and Technology, 2018, 167, 301-312.	7.8	29
308	A study of TiO ₂ nanocrystal growth and environmental remediation capability of TiO ₂ /CNC nanocomposites. RSC Advances, 2019, 9, 40565-40576.	3.6	29
309	Hierarchical Assembly of Nanocellulose into Filaments by Flow-Assisted Alignment and Interfacial Complexation: Conquering the Conflicts between Strength and Toughness. ACS Applied Materials & Interfaces, 2020, 12, 32090-32098.	8.0	29
310	In situ WAXD study of structure changes during uniaxial deformation of ethylene-based semicrystalline ethylene–propylene copolymer. Polymer, 2006, 47, 2884-2893.	3.8	28
311	Wide-Angle X-ray Scattering Study on Shear-Induced Crystallization of Propylene-1-Butylene Random Copolymer: Experiment and Diffraction Pattern Simulation. Macromolecules, 2011, 44, 558-565.	4.8	28
312	Control of structure and morphology of highly aligned PLLA ultrafine fibers via linear-jet electrospinning. Polymer, 2013, 54, 6045-6051.	3.8	28
313	Nanoparticle–Nanofibrous Membranes as Scaffolds for Flexible Sweat Sensors. ACS Sensors, 2016, 1, 1060-1069.	7.8	28
314	Operation of proton exchange membrane (PEM) fuel cells using natural cellulose fiber membranes. Sustainable Energy and Fuels, 2019, 3, 2725-2732.	4.9	28
315	Time-resolved isothermal crystallization of absorbable PGA-co-PLA copolymer by synchrotron small-angle X-ray scattering and wide-angle X-ray diffraction. Polymer, 2001, 42, 8965-8973.	3.8	27
316	Acceleration or retardation to crystallization if liquid–liquid phase separation occurs: Studies on a polyolefin blend by SAXS/WAXD, DSC and TEM. Polymer, 2007, 48, 6668-6680.	3.8	27
317	Crystal Morphology and Phase Identifications in Poly(aryl ether ketone)s and Their Copolymers. 2. Poly(oxy-1,4-phenylenecarbonyl-1,3-phenylenecarbonyl-1,4-phenylenene). Macromolecules, 1994, 27, 5787-5793.	4.8	26
318	Miscibility and phase properties of poly(aryl ether ketone)s with three high temperature all-aromatic thermoplastic polyimides. Polymer, 1996, 37, 445-453.	3.8	26
319	Primary Nucleation in Polymer Crystallization. Macromolecular Rapid Communications, 2001, 22, 611-615.	3.9	26
320	Structural and morphological development in poly(ethylene-co-hexene) and poly(ethylene-co-butylene) blends due to the competition between liquid–liquid phase separation and crystallization. Polymer, 2005, 46, 2675-2684.	3.8	26
321	Hierarchical Nanostructures of Bent-Core Molecules Blended with Poly(styrene-b-4-vinylpyridine) Block Copolymer. Macromolecules, 2007, 40, 5095-5102.	4.8	26
322	Membrane Bioreactors for Nitrogen Removal from Wastewater: A Review. Journal of Environmental Engineering, ASCE, 2020, 146, .	1.4	26
323	Cellulose nanofibrils and nanocrystals in confined flow: Single-particle dynamics to collective alignment revealed through scanning small-angle x-ray scattering and numerical simulations. Physical Review E, 2020, 101, 032610.	2.1	26
324	Nitro-oxidized carboxycellulose nanofibers from moringa plant: effective bioadsorbent for mercury removal. Cellulose, 2021, 28, 8611-8628.	4.9	26

#	Article	IF	CITATIONS
325	Simple on-line x-ray setup to monitor structural changes during fiber processing. Journal of Applied Polymer Science, 1996, 62, 2061-2068.	2.6	25
326	Aligned and molecularly oriented semihollow ultrafine polymer fiber yarns by a facile method. Journal of Polymer Science, Part B: Polymer Physics, 2010, 48, 1118-1125.	2.1	25
327	Spatial Distribution of γ-Crystals in Metallocene-Made Isotactic Polypropylene Crystallized under Combined Thermal and Flow Fields. Journal of Physical Chemistry B, 2010, 114, 6806-6816.	2.6	25
328	High-performance nanofibrous membrane for removal of Cr(VI) from contaminated water. Journal of Plastic Film and Sheeting, 2015, 31, 379-400.	2.2	25
329	Synthesis and Characterization of a High Flux Nanocellulose–Cellulose Acetate Nanocomposite Membrane. Membranes, 2019, 9, 70.	3.0	25
330	Heparinized thin-film composite membranes with sub-micron ridge structure for efficient hemodialysis. Journal of Membrane Science, 2020, 599, 117706.	8.2	25
331	Crystallization and phase behavior in nylon 6/aromatic polyimide triblock copolymers. Macromolecular Chemistry and Physics, 1998, 199, 1107-1118.	2.2	24
332	Synchrotron SAXS/WAXD and rheological studies of clay suspensions in silicone fluid. Journal of Colloid and Interface Science, 2003, 266, 339-345.	9.4	24
333	Polymer nanocomposites based on transition metal ion modified organoclays. Polymer, 2007, 48, 827-840.	3.8	24
334	Structure Development during Stretching and Heating of Isotactic Propylene–1-Butylene Random Copolymer: From Unit Cells to Lamellae. Macromolecules, 2012, 45, 7061-7071.	4.8	24
335	Biomimetic Nanofibrillation in Two-Component Biopolymer Blends with Structural Analogs to Spider Silk. Scientific Reports, 2016, 6, 34572.	3.3	24
336	Super-hydrophobic polyurethane sponges for oil absorption. Separation Science and Technology, 2017, 52, 221-227.	2.5	24
337	Interpenetrating Nanofibrous Composite Membranes for Water Purification. ACS Applied Nano Materials, 2019, 2, 3606-3614.	5.0	24
338	Reinforcement of Natural Rubber Latex Using Jute Carboxycellulose Nanofibers Extracted Using Nitro-Oxidation Method. Nanomaterials, 2020, 10, 706.	4.1	24
339	Morphology development during isothermal crystallization. II. Isotactic and syndiotactic polypropylene blends. Journal of Polymer Science, Part B: Polymer Physics, 2001, 39, 1876-1888.	2.1	23
340	Time-resolved crystallization study of absorbable polymers by synchrotron small-angle X-ray scattering. Journal of Polymer Science, Part B: Polymer Physics, 2001, 39, 153-167.	2.1	23
341	Combined techniques of Raman spectroscopy and synchrotron two-dimensional x-ray diffraction forin situstudy of anisotropic system: Example of polymer fibers under deformation. Review of Scientific Instruments, 2003, 74, 3087-3092.	1.3	22
342	Deformation behavior of oriented β-crystals in injection-molded isotactic polypropylene by in situ X-ray scattering. Polymer, 2016, 84, 254-266.	3.8	22

#	Article	IF	CITATIONS
343	Nanocomposite Film Containing Fibrous Cellulose Scaffold and Ag/TiO2 Nanoparticles and Its Antibacterial Activity. Polymers, 2018, 10, 1052.	4.5	22
344	Nanostructure Evolution of Isotropic High-Pressure Injection-Molded UHMWPE during Heating. Macromolecules, 2002, 35, 2200-2206.	4.8	21
345	Trilayer Crystalline Lamellar Morphology under Confinement. Macromolecules, 2006, 39, 2739-2742.	4.8	21
346	Synchrotron X-Ray Studies of Vulcanized Rubbers and Thermoplastic Elastomers. Rubber Chemistry and Technology, 2006, 79, 460-488.	1.2	21
347	The role of multi-walled carbon nanotubes in shear enhanced crystallization of isotactic poly(1-butene). Journal of Thermal Analysis and Calorimetry, 2009, 98, 611-622.	3.6	21
348	Orientated crystallization in discontinuous aramid fiber/isotactic polypropylene composites under shear flow conditions. Journal of Applied Polymer Science, 2005, 98, 1113-1118.	2.6	20
349	Lamellar nanostructure in 'Somasif'-based organoclays. Clays and Clay Minerals, 2007, 55, 140-150.	1.3	20
350	Influence of LC Content on the Phase Structures of Side-Chain Liquid Crystalline Block Copolymers with Bent-Core Mesogens. Macromolecules, 2009, 42, 3510-3517.	4.8	20
351	Morphological and property investigations of carboxylated cellulose nanofibers extracted from different biological species. Cellulose, 2015, 22, 3127-3135.	4.9	20
352	Fabrication of cellulose nanofiberâ€based ultrafiltration membranes by spray coating approach. Journal of Applied Polymer Science, 2017, 134, .	2.6	20
353	Nanostructured all-cellulose membranes for efficient ultrafiltration of wastewater. Journal of Membrane Science, 2022, 650, 120422.	8.2	20
354	Miscibility of three different poly(aryl ether ketones) with a high melting thermoplastic polyimide. Polymer, 1993, 34, 3315-3318.	3.8	19
355	In situ synchrotron SAXS/WAXD studies during melt spinning of modified carbon nanofiber and isotactic polypropylene nanocomposite. Colloid and Polymer Science, 2004, 282, 802-809.	2.1	19
356	Enhanced anti-fouling performance in Membrane Bioreactors using a novel cellulose nanofiber-coated membrane. Separation and Purification Technology, 2021, 275, 119145.	7.9	19
357	Lattice Deformation of Strain-induced Crystallites in Carbon-filled Natural Rubber. Chemistry Letters, 2004, 33, 220-221.	1.3	18
358	Rupture, orientation and strain-induced crystallization of polymer chain and network in vulcanized polyisoprene during uniaxial deformation by in-situ Electron Spin Resonance (ESR) and synchrotron X-ray analysis. Polymer, 2011, 52, 2453-2459.	3.8	18
359	Morphology and Flow Behavior of Cellulose Nanofibers Dispersed in Glycols. Macromolecules, 2019, 52, 5499-5509.	4.8	18
360	Structural characterization of carboxyl cellulose nanofibers extracted from underutilized sources. Science China Technological Sciences, 2019, 62, 971-981.	4.0	18

#	Article	IF	CITATIONS
361	Surfaceâ€Mediated Interconnections of Nanoparticles in Cellulosic Fibrous Materials toward 3D Sensors. Advanced Materials, 2020, 32, e2002171.	21.0	18
362	Sustainable carboxylated cellulose filters for efficient removal and recovery of lanthanum. Environmental Research, 2020, 188, 109685.	7.5	18
363	Confined Discotic Liquid Crystalline Self-Assembly in a Novel Coilâ^'Coilâ^'Disk Triblock Oligomer. Macromolecules, 2005, 38, 3386-3394.	4.8	17
364	Relationship between structure and dynamic mechanical properties of a carbon nanofiber reinforced elastomeric nanocomposite. Polymer, 2006, 47, 6797-6807.	3.8	17
365	Small-angle X-ray study of the three-dimensional collagen/mineral superstructure in intramuscular fish bone. Journal of Applied Crystallography, 2007, 40, s666-s668.	4.5	17
366	Suppressing of Î ³ -Crystal Formation in Metallocene-Based Isotactic Polypropylene during Isothermal Crystallization under Shear Flow. Journal of Physical Chemistry B, 2012, 116, 5056-5063.	2.6	17
367	Crystalline Structure Changes in Preoriented Metallocene-Based Isotactic Polypropylene upon Annealing. Journal of Physical Chemistry B, 2013, 117, 7113-7122.	2.6	17
368	Improving toughness of ultra-high molecular weight polyethylene with ionic liquid modified carbon nanofiber. Polymer, 2014, 55, 160-165.	3.8	17
369	Structure and permeability relationships in polymer nanocomposites containing carbon black and organoclay. Polymer, 2015, 64, 19-28.	3.8	17
370	Modification of carbon nanotubes with fluorinated ionic liquid for improving processability of fluoro-ethylene-propylene. European Polymer Journal, 2017, 87, 398-405.	5.4	17
371	Ionic Cross-Linked Poly(acrylonitrile- <i>co</i> -acrylic acid)/Polyacrylonitrile Thin Film Nanofibrous Composite Membrane with High Ultrafiltration Performance. Industrial & Engineering Chemistry Research, 2017, 56, 3077-3090.	3.7	17
372	High-flux anti-fouling nanofibrous composite ultrafiltration membranes containing negatively charged water channels. Journal of Membrane Science, 2020, 612, 118382.	8.2	17
373	Time-resolved simultaneous SAXS/WAXS studies of peek during isothermal crystallization, melting, and subsequent cooling. Journal of Macromolecular Science - Physics, 1998, 37, 667-682.	1.0	16
374	Inducing Order from Disordered Copolymers: On Demand Generation of Triblock Morphologies Including Networks. Macromolecules, 2012, 45, 4599-4605.	4.8	16
375	Copolymer modification of nylon-6,6 with 2-methylpentamethylenediamine. Polymer, 1996, 37, 1217-1228.	3.8	15
376	Morphological Changes during the Annealing of Polybutene-1 Fiber. Macromolecules, 2001, 34, 2008-2011.	4.8	15
377	Flow-induced crystallization precursor structure in high molecular weight isotactic polypropylene (HMW-iPP)/low molecular weight linear low density polyethylene (LMW-LLDPE) binary blends. Polymer, 2013, 54, 1425-1431.	3.8	15
378	A novel way to monitor the sequential destruction of parent-daughter crystals in isotactic polypropylene under uniaxial tension. Journal of Materials Science, 2014, 49, 3016-3024.	3.7	15

#	Article	IF	CITATIONS
379	Probing structure and orientation in polymers using synchrotron small- and wide-angle X-ray scattering techniques. European Polymer Journal, 2016, 81, 433-446.	5.4	15
380	Decoration of Nanofibrous Paper Chemiresistors with Dendronized Nanoparticles toward Structurally Tunable Negativeâ€Going Response Characteristics to Human Breathing and Sweating. Advanced Materials Interfaces, 2017, 4, 1700380.	3.7	15
381	Enhancing Dehydration Performance of Isopropanol by Introducing Intermediate Layer into Sodium Alginate Nanofibrous Composite Pervaporation Membrane. Advanced Fiber Materials, 2019, 1, 137-151.	16.1	15
382	Study of a thermotropic liquid-crystalline polyester at elevated pressures. Journal of Polymer Science, Part B: Polymer Physics, 1990, 28, 189-202.	2.1	14
383	Reversible De-Intercalation and Intercalation Induced by Polymer Crystallization and Melting in a Poly(ethylene oxide)/Organoclay Nanocomposite. Langmuir, 2005, 21, 5672-5676.	3.5	14
384	DEPENDENCE OF THE ONSET OF STRAIN-INDUCED CRYSTALLIZATION OF NATURAL RUBBER AND ITS SYNTHETIC ANALOGUE ON CROSSLINK AND ENTANGLEMENT BY USING SYNCHROTRON X-RAY. Rubber Chemistry and Technology, 2017, 90, 728-742.	1.2	14
385	An unusual promotion of γ-crystals in metallocene-made isotactic polypropylene from orientational relaxation and favorable temperature window induced by shear. Polymer, 2018, 134, 196-203.	3.8	14
386	Influences of tacticity and molecular weight on crystallization kinetic and crystal morphology under isothermal crystallization: Evidence of tapering in lamellar width. Polymer, 2019, 172, 41-51.	3.8	14
387	Crystal structure changes during isothermal crystallization, cooling and heating of linear polyethylene. Journal of Polymer Research, 1999, 6, 167-173.	2.4	13
388	Chain-Folding and Overall Molecular Conformation in a Novel Amphiphilic Starlike Macromolecule. Macromolecules, 2005, 38, 7074-7082.	4.8	13
389	Sequence distribution and elastic properties of propylene-based elastomers. Polymer, 2017, 111, 115-122.	3.8	13
390	The influence of short chain branch on formation of shear induced crystals in bimodal polyethylene at high shear temperatures. European Polymer Journal, 2018, 105, 359-369.	5.4	13
391	Electrospun Nanofibrous Membranes for Desalination. , 2019, , 81-104.		13
392	Morphological Changes During Crystallization and Melting of Polyoxymethylene Studied by Synchrotron X-Ray Scattering and Modulated Differential Scanning Calorimetry. Journal of Macromolecular Science - Physics, 2000, 39, 519-543.	1.0	12
393	A Synchrotron WAXD Study on the Early Stages of Coagulation during PBO Fiber Spinning. Macromolecules, 2002, 35, 9851-9853.	4.8	12
394	Structure and morphology development during deformation of propylene based ethylene–propylene copolymer and its blends with isotactic polypropylene. Polymer, 2003, 44, 2385-2392.	3.8	12
395	Uniaxial Deformation of Nylon 6–Clay Nanocomposites by In-Situ Synchrotron X-Ray Measurements. Journal of Macromolecular Science - Physics, 2003, 42, 201-214.	1.0	12
396	Development of Multiple-Jet Electrospinning Technology. ACS Symposium Series, 2006, , 91-105.	0.5	12

#	Article	IF	CITATIONS
397	The role of high molecular weight chains in flow-induced crystallization precursor structures. Journal of Physics Condensed Matter, 2006, 18, S2421-S2436.	1.8	12
398	Structure Evolution upon Uniaxial Drawing Skin―and Coreâ€Layers of Injectionâ€Molded Isotactic Polypropylene by <i>In Situ</i> Synchrotron Xâ€ray Scattering. Journal of Polymer Science, Part B: Polymer Physics, 2013, 51, 1618-1631.	2.1	12
399	Effects of molecular geometry on the self-assembly of giant polymer–dendron conjugates in condensed state. Soft Matter, 2014, 10, 3200.	2.7	12
400	A Criterion for Flowâ€Induced Oriented Crystals in Isotactic Polypropylene under Pressure. Macromolecular Rapid Communications, 2017, 38, 1700407.	3.9	12
401	The influence of short chain branch on formation of shishâ€kebab crystals in bimodal polyethylene under shear at high temperatures. Journal of Polymer Science, Part B: Polymer Physics, 2018, 56, 786-794.	2.1	12
402	Solvent induced phase separation in a nylon 6-b-polyimide-b-nylon 6 triblock copolymer. Journal of Polymer Research, 1997, 4, 1-7.	2.4	11
403	A new pathway for developingin vitronanostructured non-viral gene carriers. Journal of Physics Condensed Matter, 2006, 18, S2513-S2525.	1.8	11
404	Crystallization behavior of isotactic propyleneâ€1â€hexene random copolymer revealed by timeâ€resolved SAXS/WAXD techniques. Journal of Polymer Science, Part B: Polymer Physics, 2010, 48, 26-32.	2.1	11
405	Nanocellulose Extracted from Defoliation of Ginkgo Leaves. MRS Advances, 2018, 3, 2077-2088.	0.9	11
406	Nitro-oxidized carboxylated cellulose nanofiber based nanopapers and their PEM fuel cell performance. Sustainable Energy and Fuels, 2022, 6, 3669-3680.	4.9	11
407	Structural and Morphological Inhomogeneity of Short-Chain Branched Polyethylenes in Multiple-Step Crystallization. Journal of Macromolecular Science - Physics, 2000, 39, 317-331.	1.0	10
408	Salt-Induced Polymer Gelation and Formation of Nanocrystals in a Polymerâ^'Salt System. Langmuir, 2002, 18, 10402-10406.	3.5	10
409	Fabrication of Micro-Nano Structure Nanofibers by Solvent Etching. Journal of Nanoscience and Nanotechnology, 2011, 11, 6919-6925.	0.9	10
410	Polymeric nanofibrous composite membranes for energy efficient ethanol dehydration. Journal of Renewable and Sustainable Energy, 2012, 4, .	2.0	10
411	Microstructure and mechanical properties of isotactic polypropylene composite with twoâ€scale reinforcement. Polymers for Advanced Technologies, 2012, 23, 1580-1589.	3.2	10
412	Current Advances on Nanofiber Membranes for Water Purification Applications. , 2018, , 25-46.		10
413	The influence of short chain branch on formation of shear-induced crystals in bimodal polyethylene at low shear temperatures. Polymer, 2019, 179, 121625.	3.8	9
414	Ordering kinetics of body-centered-cubic morphology in diblock copolymer solutions at low temperatures. Journal of Rheology, 2004, 48, 1389-1405.	2.6	8

#	Article	IF	CITATIONS
415	Rheological Properties of Jute-Based Cellulose Nanofibers under Different Ionic Conditions. ACS Symposium Series, 2017, , 113-132.	0.5	8
416	Functionalized bioâ€adsorbents for removal of perfluoroalkyl substances: A perspective. AWWA Water Science, 2021, 3, .	2.1	8
417	Anomalous two-stage spherulite growth in poly(aryl ether ketones) during isothermal crystallization. Journal of Polymer Science, Part B: Polymer Physics, 1996, 34, 3095-3105.	2.1	7
418	Crystallization study of poly(ether ether ketone)/poly(ether imide) blends by real-time small-angle x-ray scattering. Journal of Macromolecular Science - Physics, 1998, 37, 365-374.	1.0	7
419	Probing the flow-induced shish-kebab structure in entangled polyethylene melts by synchrotron X-ray scattering. Journal of Applied Crystallography, 2006, 40, s48-s51.	4.5	7
420	Sulfonylcalix[4]arene functionalized nanofiber membranes for effective removal and selective fluorescence recognition of terbium(<scp>iii</scp>) ions. New Journal of Chemistry, 2018, 42, 6191-6202.	2.8	7
421	Remediation of UO ₂ ²⁺ from Water by Nitro-Oxidized Carboxycellulose Nanofibers: Performance and Mechanism. ACS Symposium Series, 2020, , 269-283.	0.5	7
422	Electrospun Nanofibrous Adsorption Membranes for Wastewater Treatment: Mechanical Strength Enhancement. Chemical Research in Chinese Universities, 2021, 37, 355-365.	2.6	7
423	Role of Chain Entanglement Network on Formation of Flow-Induced Crystallization Precursor Structure. , 2007, , 133-149.		7
424	Crystal Morphology and Phase Identification in Poly(Aryl Ether Ketone)s and Their Copolymers. 4. Morphological Observations in PEKK with All p-Phenylene Linkages. Macromolecules, 1995, 28, 8855-8861.	4.8	6
425	Synchrotron X-ray scattering studies of the nature of shear-induced shish-kebab structure in polyethylene melt. , 2005, , 114-126.		6
426	The effect of comonomer content on structure and property relationship of propylene-1-octene copolymer during uniaxial stretching. Polymer, 2013, 54, 4545-4554.	3.8	6
427	Morphology and mechanical properties of heterophasic PP–EP/EVA/organoclay nanocomposites. Journal of Applied Polymer Science, 2013, 128, 3473-3479.	2.6	6
428	Nanoparticle Based Printed Sensors on Paper for Detecting Chemical Species. , 2017, , .		6
429	Shear induced crystallization of bimodal and unimodal high density polyethylene. Polymer, 2018, 153, 223-231.	3.8	6
430	Shear-free mixing to achieve accurate temporospatial nanoscale kinetics through scanning-SAXS: ion-induced phase transition of dispersed cellulose nanocrystals. Lab on A Chip, 2021, 21, 1084-1095.	6.0	6
431	Nano-Filamented Textile Sensor Platform with High Structure Sensitivity. ACS Applied Materials & Interfaces, 2022, 14, 15391-15400.	8.0	6
432	Time-resolved synchrotron X-ray study of crystalline phase transition in poly(aryl ether ketone) Tj ETQq0 0 0 rgE Polymer Physics, 1995, 33, 2439-2447.	T /Overloc 2.1	k 10 Tf 50 67 5

#	Article	IF	CITATIONS
433	Melt crystalfization and crystal morphology of two low molecular weight linear polyethylene fractions. Journal of Macromolecular Science - Physics, 1997, 36, 553-567.	1.0	5
434	Crystal morphological investigation in thin films of poly(aryl ether ketone ketone) having a meta-linkage. Polymer, 1997, 38, 5051-5058.	3.8	5
435	Synchrotron Xâ€Ray scattering of polymer nanocomposites. Synchrotron Radiation News, 2002, 15, 20-34.	0.8	5
436	Shear Enhanced Crystallization and Tensile Behaviors of Oscillation Shear Injection Molded Poly(ethylene terephthalate). Journal of Macromolecular Science - Physics, 2010, 50, 383-397.	1.0	5
437	Development of internal fine structure in stretched rubber vulcanizates. Journal of Polymer Science, Part B: Polymer Physics, 2011, 49, 1157-1162.	2.1	5
438	High-pressure crystallization of poly(lactic acid) with and without N2 atmosphere protection. Journal of Materials Science, 2013, 48, 7374-7383.	3.7	5
439	The supramolecular structure of bone: X-ray scattering analysis and lateral structure modeling. Acta Crystallographica Section D: Structural Biology, 2016, 72, 986-996.	2.3	5
440	Comprehensive study on temperature-induced crystallisation and strain-induced crystallisation behaviours of natural rubber/isoprene rubber blends. Plastics, Rubber and Composites, 2017, 46, 290-300.	2.0	5
441	Sequential Oxidation on Wood and Its Application in Pb2+ Removal from Contaminated Water. Polysaccharides, 2021, 2, 245-256.	4.8	5
442	Understanding ion-induced assembly of cellulose nanofibrillar gels through shear-free mixing and in situ scanning-SAXS. Nanoscale Advances, 2021, 3, 4940-4951.	4.6	5
443	Study the Use of Activated Carbon and Bone Char on the Performance of Gravity Sand-Bag Water Filter. Membranes, 2021, 11, 868.	3.0	5
444	Anomalous rheology in a nanostructured diblock copolymer/hydrocarbon system and its kinetic origin. Journal of Polymer Science, Part B: Polymer Physics, 2004, 42, 1496-1505.	2.1	4
445	Deformation X-ray study of propylene-based elastomers with controlled sequence distributions. Polymer, 2017, 122, 208-221.	3.8	4
446	Colorful nanofibrous composite membranes by two-nozzle electrospinning. Materials Today Communications, 2019, 21, 100643.	1.9	4
447	The Influence of Ethyl Branch on Formation of Shish-Kebab Crystals in Bimodal Polyethylene under Shear at Low Temperature. Chinese Journal of Polymer Science (English Edition), 2021, 39, 1050-1058.	3.8	4
448	Electrospun Nanofibrous Membranes for Liquid Filtration. Nanostructure Science and Technology, 2014, , 325-354.	0.1	3
449	Shear-induced crystallization of unimodal/bimodal polyethylene at high temperatures affected by C4 short-branching. Polymer, 2021, 233, 124203.	3.8	3

#	Article	IF	CITATIONS
451	The Effects of Temperature and Pressure on the Dynamic Longitudinal Volume Viscosity of Two Model Polymers. Journal of Rheology, 1988, 32, 533-553.	2.6	2
452	Crystallization and structure formation in polymer blends with strong intermodular interactions: blends of poly(ethylene oxide) and styrene-hydroxystyrene copolymers. Macromolecular Symposia, 2003, 198, 29-40.	0.7	2
453	Deformation-Induced Structure Changes in Elastomeric Nanocomposites. Advanced Structured Materials, 2011, , 135-154.	0.5	2
454	CHEMICAL APPLICATIONS OF SMALL ANGLE SCATTERING. Advanced Series in Physical Chemistry, 2002, , 799-849.	1.5	1
455	Continuous Production of Hollow Hydrogel Fibers with Graphene Inner Wall. Materials Science Forum, 0, 898, 2197-2204.	0.3	1
456	A thirst for advancement. Nature Materials, 2018, 17, 213-215.	27.5	1
457	Effect of Sorbitol Templates on the Preferential Crystallographic Growth of Isotactic Polypropylene Wax. Crystals, 2018, 8, 59.	2.2	1
458	Crystal structural evolution of Polybutene-1 in solid state upon deformation and stress relaxation. Polymer, 2021, 226, 123833.	3.8	1
459	Lamellar crystal-dominated surfaces of polymer films achieved <i>via</i> melt stretching-induced free surface crystallization. Soft Matter, 2021, 17, 10829-10838.	2.7	1
460	Microstructure and Phase Separation of Pekk, Pekk and their Blends. Materials Research Society Symposia Proceedings, 1996, 461, 33.	0.1	0
461	Self-Bundling Electrospinning Method. , 2013, , 1-2.		Ο
462	Nanoclays. , 2013, , 1-2.		0
463	Benzyl-Modified Cellulose. , 2014, , 1-2.		Ο
464	Ultrafine Nanofibers. , 2016, , 1951-1953.		0
465	Self-Bundling Electrospinning Method. , 2016, , 1762-1763.		Ο
466	Nanocellulose in membrane technology for water purification. Separation Science and Technology, 2022, , 69-85.	0.2	0
467	Plant-derived carboxycellulose: Highly efficient bionanomaterials for removal of toxic lead from contaminated water. Separation Science and Technology, 2022, , 87-95.	0.2	0
468	Nitro-oxidation process for fabrication of efficient bioadsorbent from lignocellulosic biomass by combined liquid-gas phase treatment. Carbohydrate Polymer Technologies and Applications, 2022, 3, 100219.	2.6	0